Analytical and Bioanalytical Chemistry
https://doi.org/10.1007/s00216-018-1439-2

RESEARCH PAPER

A MnO_2 nanosheet-based ratiometric fluorescent nanosensor with single excitation for rapid and specific detection of ascorbic acid

Yanlong Lyu[1] · Zhanhui Tao[1] · Xiaodong Lin[1] · Pengcheng Qian[1] · Yunfei Li[1] · Shuo Wang[2] · Yaqing Liu[1]

Received: 30 July 2018 / Revised: 25 September 2018 / Accepted: 19 October 2018

Abstract

Ascorbic acid (AA) detection in biological sample and food sample is critical for human health. Herein, a MnO_2 nanosheet (MnO_2-NS)-based ratiometric fluorescent nanosensor has been developed for high sensitive and specific detection of AA. The MnO_2-NS presents peroxidase-like activity and can oxidize non-fluorescent substrate of *o*-phenylenediamine (OPDA) into fluorescent substrate, presenting maximum fluorescence at 568 nm (F_{568}). If MnO_2-NS is premixed with AA, the MnO_2-NS is then decomposed as Mn^{2+} by AA, decreasing the fluorescent intensity of F_{568}. Meantime, AA is oxidized as dehydroascorbic acid (DHAA), which can react with OPDA to generate fluorescent substrate. A new fluorescence response is found at 425 nm (F_{425}). The dual fluorescent responses can be excited with a universal excitation wavelength, simplifying the detection procedure. With F_{425}/F_{568} as readout, limit of detection for AA reaches as low as 10.0 nM. Satisfactory recoveries are found for AA detection in serum and diverse beverages. The ratiometric strategy significantly eliminates false-negative and false-positive results, providing a cost-effective, rapid, and reliable way for AA detection in real sample.

Keywords Ratiometric biosensor · Fluorescent biosensor · MnO_2 nanosheet · Ascorbic acid · Dual fluorescence with single excitation

Introduction

As an important micronutrient, ascorbic acid (AA) also known as vitamin C is essential to human health and plays a critical role in many biochemical processes [1–3]. It can promote formation of antibody, synthesis of collagen and neurotransmitters, and maintenance of thiolase activity for improving immunity and preventing of scurvy [4]. Meanwhile, AA acts as antioxidant to neutralize toxic peroxides in human body to reduce the risk of cancer [5]. Deficiency of AA would lead to serious diseases, for example, hypoimmunity, scurvy, mental illness, and even cancer [6, 7]. The necessary AA for human is usually obtained from external substrates such as diverse of foods, beverages, and pharmaceutical formulations since AA cannot be generated from the biosynthesis procedure in human body [8]. However, excessive AA also results in various diseases such as coronary heart disease, hyperacidity, and diarrhea [9, 10]. Therefore, it is urgent to develop a simple, rapid, and low-cost assay for AA determination in biological sample and also food sample with high sensitivity and specificity.

Up to date, detection strategies for AA have been developed according to diverse techniques including colorimetric [11], fluorimetric [12], and electrochemical methods [13], as well as liquid chromatograph [14]. Among the various detection strategies, fluorimetric assay has attracted increasing attention due to its advantages of simple in preparation and operation, low cost, and excellent sensitivity [15, 16]. Nanomaterials have been confirmed to be charming candidate for construction of enzyme-free and label-free fluorescent

Published in the topical collection *New Insights into Analytical Science in China* with guest editors Lihua Zhang, Hua Cui, and Qiankun Zhuang.

Electronic supplementary material The online version of this article (https://doi.org/10.1007/s00216-018-1439-2) contains supplementary material, which is available to authorized users.

✉ Shuo Wang
wangshuo@nankai.edu.cn

✉ Yaqing Liu
yaqingliu@tust.edu.cn

[1] State Key Laboratory of Food Nutrition and Safety, Key Laboratory of Food Nutrition and Safety (Ministry of Education), College of Food Engineering and Biotechnology, Tianjin University of Science and Technology, Tianjin 300457, China

[2] Tianjin Key Laboratory of Food Science and Health, School of Medicine, Nankai University, Tianjin 300071, China

Published online: 07 November 2018

biosensors for AA [17–20]. With fluorescent nanomaterials as signal probes, for example carbon dots, graphene quantum dots, Au nanocluster, and upconverting nanoparticles (UCNP), diverse assays have been developed for sensitive detection of AA [21–27]. In recent years, MnO_2 nanomaterials have attracted ever increasing attention for construction of enzyme-free and label-free sensors on the basis of their intrinsic advantages of excellent oxidase-like activity, high specific surface area, rich structural diversity, and unique electronic properties [28–32]. MnO_2 nanomaterials can be reduced into Mn^{2+} as a result of the redox reaction between MnO_2 and AA, guiding for AA sensors construction. Here, we noted that MnO_2 nanomaterials also can be decomposed into Mn^{2+} by glutathione (GSH), cysteine (Cys), or dopamine (DA), which was utilized for biosensor construction [33–37]. Since AA, GSH, Cys, and DA may coexist in human body, this would raise a limitation for specific detection of AA with MnO_2-based assay, which is usually ignored in previous investigations [26]. Meanwhile, it is worthy of noting that most of the developed fluorescent biosensors for AA are based on single-signal either "turn-on" or "turn-off" strategy, which might cause false-positive or false-negative results [38]. A ratiometric sensor can outstandingly minimize the interfering environment or background factors by recording the fluorescence intensity ratio of two different emission bands, presenting built-in correction function. Thus the sensing accuracy and reliability can be significantly improved [39]. Inspired by this, herein, we developed a novel ratiometric MnO_2-based biosensor for high sensitive and selective detection of AA, eliminating the interference from GSH, Cys, and DA.

Experimental section

Materials and chemicals

o-Phenylenediamine (OPDA) was purchased from TCI (Shanghai) Development Co., Ltd. Ethanesulfonic acid (MES) was purchased from Beijing Solarbio Science & Technology Co., Ltd. Sodium dihydrogen phosphate (NaH_2PO_4), disodium hydrogen phosphate (Na_2HPO_4), ascorbic acid (AA), $KMnO_4$, glucose, dopamine, uric acid, bovine serum albumin (BSA), GSH (reduced form), all the metal ion salts, and amino acids were purchased from Sinopharm Chemical Reagent Co., Ltd. All the used chemicals are of analytical reagent without further purification. All solutions were prepared with ultrapure water obtained from Milli-Q purification system. Phosphate buffer (PB) solution (pH 6.5, 25 mM) was used as the medium for the detection. All of the beverage samples for real sample detection were purchased from a local supermarket in Tianjin, China. Fetal bovine serum was purchased from Scitecher and was filtered (0.1 mm) by the manufacturer prior to purchase.

Apparatus

Ultraviolet-visible (UV-Vis) spectra were recorded with a Cary 50-Bio UV spectrometer (Victoria, Australia). Fluorescence spectra were recorded with a LUMINA Fluorescence Spectrometer (Thermo, USA). Transmission electron microscopy (TEM) images were obtained with a 2010FEF microscope (JEOL, Japan).

Synthesis of MnO_2 nanosheet

MnO_2 nanosheet (MnO_2-NS) was synthesized according to previous report with minor modification [40]. Briefly, MnO_2-NS was prepared by following a sonication-induced reduction of $KMnO_4$ in MES buffer. $KMnO_4$ (500 μL, 10.0 mM) solution was added into MES buffer solution (1.25 mL, 0.1 M, pH 6.0). The final volume was adjusted to 5.0 mL by water. After sonicating for 30 min, the MnO_2-NS was obtained by centrifugation at (15,294 rcf) for 10 min following water-wash for three times to remove the excess potassium and manganese ions. The as-prepared MnO_2-NS was redispersed into 5 mL water for the following studies. Using the molar extinction coefficient of $9.6 \times 10^3\ M^{-1}\ cm^{-1}$ (380 nm) [28, 29], the calculated concentration of the prepared MnO_2 nanosheet was 4.5 mM. The solution of final concentration was diluted to 1.0 mM for the following experiment. The as-prepared MnO_2 nanomaterial presented well water solubility and was characterized with transmission electron microscopy, indicating the successful preparation of ultrathin MnO_2 nanosheets (see Fig. S1 in Electronic Supplementary Material (ESM)).

Fluorescent detection of AA

MnO_2-NS (1.0 mM, 30 μL) and AA (100 μM) were mixed and then diluted into 200 μL with PB buffer (pH = 6.5, 25 mM). The final concentrations of AA were 0.0, 0.05, 0.1, 0.5, 1.0, 2.0, 3.0, 5.0, and 6.0 μM. After incubating 5 min, OPDA (10 mM, 20 μL) was then added into the mixture. After incubating for 20, the fluorescence intensities of the two fluorescent signals were detected with a fluorescence spectrophotometer under universal excitation (λ_{em} = 360 nm).

Selectivity

Taking the complex environment into consideration, the interfering substances were selected for mainly organism amino acids and small molecules and metal ions with physiological concentrations: ascorbic acid (10 μM), glycine (Gly), glutamic acid (Glu), arginine (Arg), lysine (Lys), proline (Pro), histidine (His), cysteine (Cys), glutathione (GSH), glucose (GLU), dopamine (DA), BSA, uric acid (UA), calcium ion (Ca^{2+}), sodium ion (Na^{+}), zinc ion (Zn^{2+}), copper ion (Cu^{2+}), and iron ion (Fe^{3+}) were used as the interfering

substances. The interfering substances were all 20 μM. After incubating with the sensing system, the fluorescence responses were measured via fluorescence spectrophotometer.

AA detection in real samples

Commercial fruit juices, i.e., orange juice, lemon juice, grapefruit juice, and pineapple juice, were centrifuged for 20 min (1157 rcf) in a refrigerated centrifuge (4 °C). The supernatant was filtered through a 0.45-μm pore size filter membrane. Serum was centrifuged for 5 min (4629 rcf) and then separated. The initial concentrations of AA in the above samples were detected with HPLC method by following national standard testing method (GB500986-2016, China). After being diluted into an appropriate concentration with ultrapure water, AA with different concentrations was spiked into the real samples, which was detected following the as-provided ratiometric strategy.

Results and discussion

Detection principle and feasibility for ascorbic acid detection

Scheme 1 outlines the principle for ratiometric detection of ascorbic acid. The ratiometric sensing system was constructed on the basis of the competitive reaction among MnO_2-NS, AA, and OPDA. Briefly, the non-fluorescent substrate of OPDA can be oxidized into fluorescent substrate of 2,3-diaminophenazine (OPDAox), presenting maximum fluorescence at 568 nm (F_{568}). In the presence of AA, the MnO_2-NS is reduced into Mn^{2+}, and AA is oxidized into dehydroascorbic acid (DHAA). The produced DHAA can reduce OPDA into quinoxaline, presenting fluorescence at 425 nm. It is expected that the fluorescence decreasing at 568 nm and increasing at 425 nm would be related to the ascorbic acid concentration. With the ratio of fluorescent intensity at 425 nm (F_{425}) to that at 568 nm (F_{568}) as readout signal (F_{425}/F_{568}), a fluorescent ratiometric biosensor was constructed for AA detection.

Absorption and fluorescent spectra were monitored to validate the feasibility of the developed strategy (Fig. 1). As control experiments, no obvious fluorescence emission is monitored from AA, OPDA, MnO_2-NS, or the mixture of MnO_2-NS and AA (Fig. 1A (a–d)). The non-fluorescent substrate of OPDA is oxidized into fluorescent substrate of OPDAox by the as-synthesized MnO_2-NS, presenting maximum fluorescent intensity at 568 nm (Fig. 1A (e)). If first incubating MnO_2-NS with AA, the MnO_2-NS is then reduced into Mn^{2+}, and AA is oxidized into DHAA according to the following reaction $MnO_2 + AA + 2H^+ \rightarrow Mn^{2+} + DHAA + 2H_2O$ [41]. With the decomposition of MnO_2-NS, the generation of OPDAox is correspondingly reduced, resulting in a decreased fluorescence of OPDAox (Fig. 1A (f)). Meanwhile, the generated DHAA interacts with OPDA to produce fluorescent substrate of quinoxaline [42], exhibiting maximum fluorescent intensity at 425 nm (Fig. 1A (f)). The interaction between MnO_2-NS and AA was further validated with the absorption experiments (Fig. 1B). After reacting with AA, the yellow solution of MnO_2-NS becomes transparent, and the maximum absorption peak of MnO_2-NS at 400 nm (curve

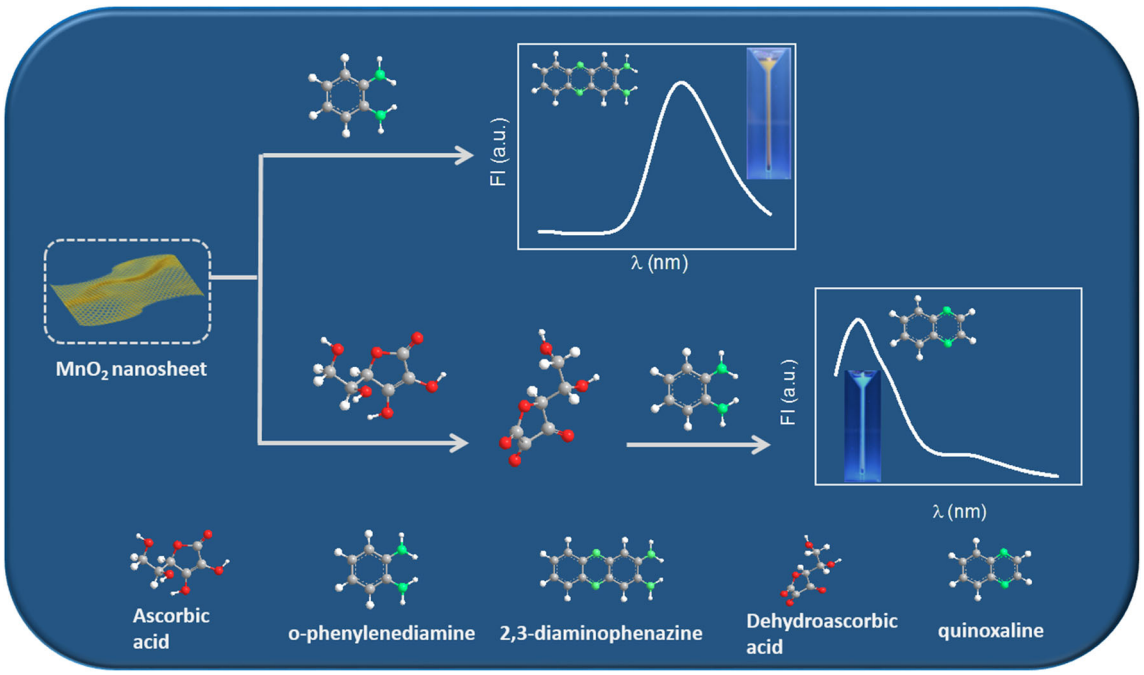

Scheme 1 Schematic mechanism of MnO_2-NS based ratiometric fluorescent nanosensor for AA detection

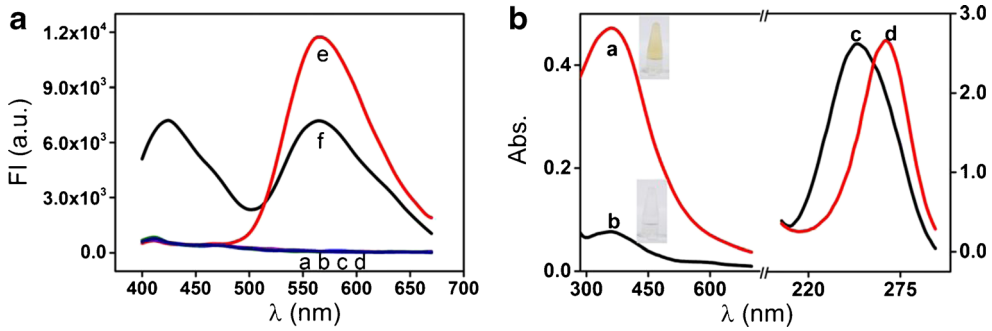

Fig. 1 (A) (a) Fluorescence spectra of AA, (b) OPDA, (c) MnO_2-NS, (d) MnO_2-NS + AA, (e) MnO_2-NS + OPDA, AA + MnO_2-NS + OPDA (f). (B) (a) UV-vis absorption spectra of MnO_2-NS, (b) MnO_2-NS + AA, (c) AA, (d) MnO_2-NS + AA. Inset: photographs of the MnO_2-NS (up) and MnO_2-NS + AA (down)

a) is significantly declined (curve b), indicating the decomposition of MnO_2-NS by AA. Meanwhile, the maximum absorption of AA at 249 nm (curve c) is shifted to 266 nm due to the generation of DHAA (curve d). The absorption results are well consistent with the fluorescent results, further confirming the feasibility of the developed detection strategy for AA.

Optimization of experimental procedure

Considering that AA detection is realized according to the competition interaction of AA and MnO_2-NS with OPDA, the concentration of MnO_2-NS is critical to the detection sensitivity. If MnO_2-NS is superfluous, more AA would be required to cause fluorescence change of the sensing system, which would reduce the sensitivity. To find the optimized concentration of MnO_2-NS, fluorescence titration experiments were conducted by adding MnO_2-NS with different concentrations into OPDA solution (Fig. 2A). The fluorescence of the produced OPDAox reaches a plateau when the concentration of MnO_2-NS is over than 0.2 mM, which is used in the following experiments. As described above, two fluorescence signals of OPDAox and quinoxaline are monitored in the mixture of MnO_2-NS, AA, and OPDA. We noted that the excitation wavelengths for OPDAox and quinoxaline are 365 nm and 355 nm, respectively, which are close to each other. To simplify the experimental operation, here, we tried to

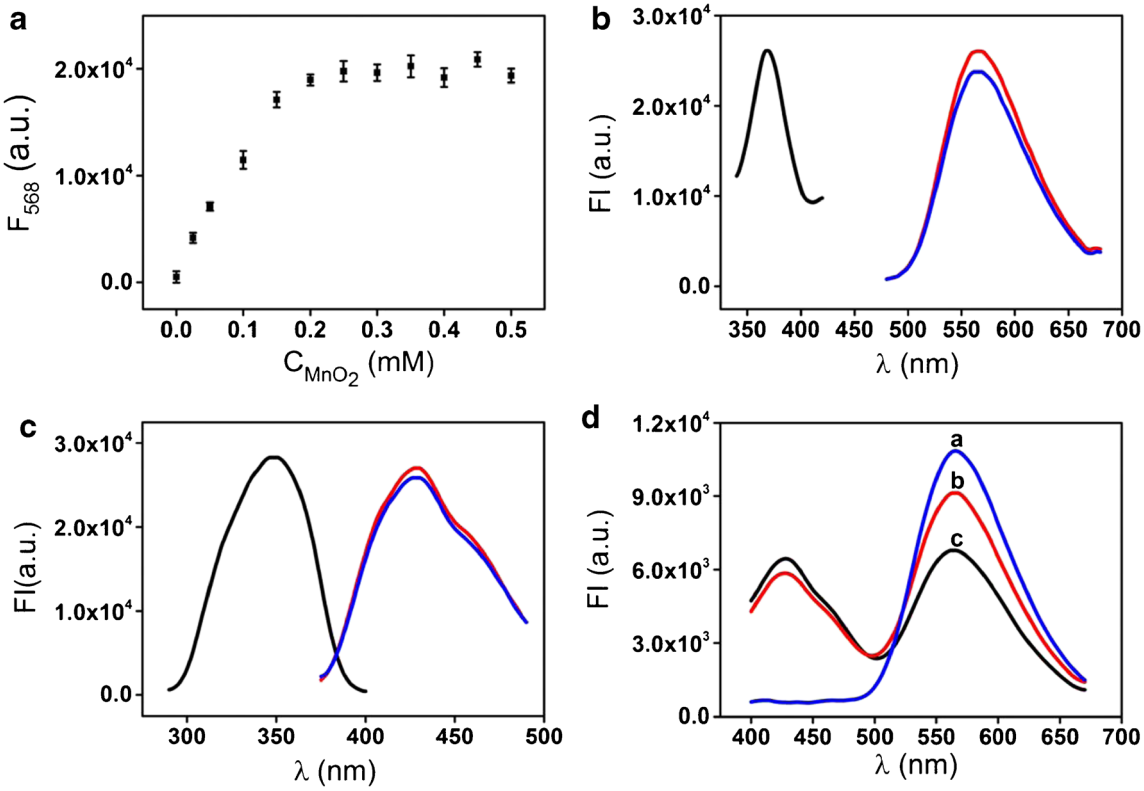

Fig. 2 (A) F_{568} of the sensing system against concentration of MnO_2-NS. (B) Fluorescence excitation (black) and emissions of OPDAox under radiation (λ_{em} = 365 nm, red) and (λ_{em} = 360 nm, blue). (C) Fluorescence emissions of quinoxaline under radiation of (λ_{em} = 355 nm, red) and (λ_{em} = 360 nm, blue). (D) (a) Fluorescence spectra of mixture of MnO_2-NS and OPDA, (b) first mixing MnO_2-NS and OPDA, following the addition of AA, and (c) first mixing MnO_2-NS and AA, following the addition of OPDA. Error bars were standard deviation and obtained from three independent experiments

used 360 nm as common excitation wavelength for both OPDAox (Fig. 2B) and quinoxaline (Fig. 2C). Interestingly, only slight decreases are monitored from fluorescences of OPDAox and quinoxaline, which has no influence on the sensitivity in following detections. Thus, 360 nm is selected as the universal excitation wavelength for the ratiometric detection of AA, further simplifying the operation. During investigation, it was found that the interaction between MnO_2-NS and OPDA is quite rapid to produce fluorescent substrate of OPDAox. Only one fluorescent response is found at 568 nm (Fig. 2D (a)). Figure 2(D (b)) represents the fluorescent response of the system if first incubating MnO_2-NS and OPDA and then adding AA. In this case, the fluorescent response at 568 nm decreases while a new fluorescent response at 425 nm appears. Figure 2(D (c)) represents the fluorescent response of the system if first incubating MnO_2-NS and AA and then adding OPDA. Compared with Fig. 2(D (b)), in this case, the system exhibits a lower fluorescent response at 568 nm and a higher fluorescent response at 425 nm, which results in a more distinguished detection signal of F_{425}/F_{568}. Therefore, the second procedure is adopted for AA detection.

Optimization of experimental condition

To improve detection sensitivity and repeatability, the incubation time was explored for obtaining a stable fluorescent response. The fluorescent responses of quinoxaline at 425 nm (Fig. 3a) and OPDAox at 568 nm (Fig. 3b) were monitored against incubation time after adding OPDA into the mixture of AA and MnO_2-NS. The fluorescent responses of quinoxaline or OPDAox reach a plateau after incubation 10 min and 20 min, respectively. Considering the interactions occurred in homogenous solution, here, 20 min is selected in the following experiments. The influence of buffer pH value was further explored. The fluorescent response of quinoxaline keeps relatively stable from pH 5.0 to 6.5 and then decreases in base solution (Fig. 3c). The fluorescent response of OPDAox has slight increase from pH 5.0 to 7.0 and then gradually decreases from pH 7.0 to 8.0, which is greatly quenched at pH 8.5 (Fig. 3d). Thus, pH 6.5 is used in the following experiments.

Sensitivity of the developed sensing system

Under the optimal experimental conditions, the sensitivity of the developed ratiometric fluorescent assay was evaluated by monitoring the fluorescence response of the sensing system as a function of AA concentration (Fig. 4). In the absence of AA, only fluorescence of OPDAox with maximum emission at 568 nm is monitored. With the addition of AA, the fluorescence spectrum of the sensing system is changed from a single peak into dual peaks. Due to the interaction between AA and

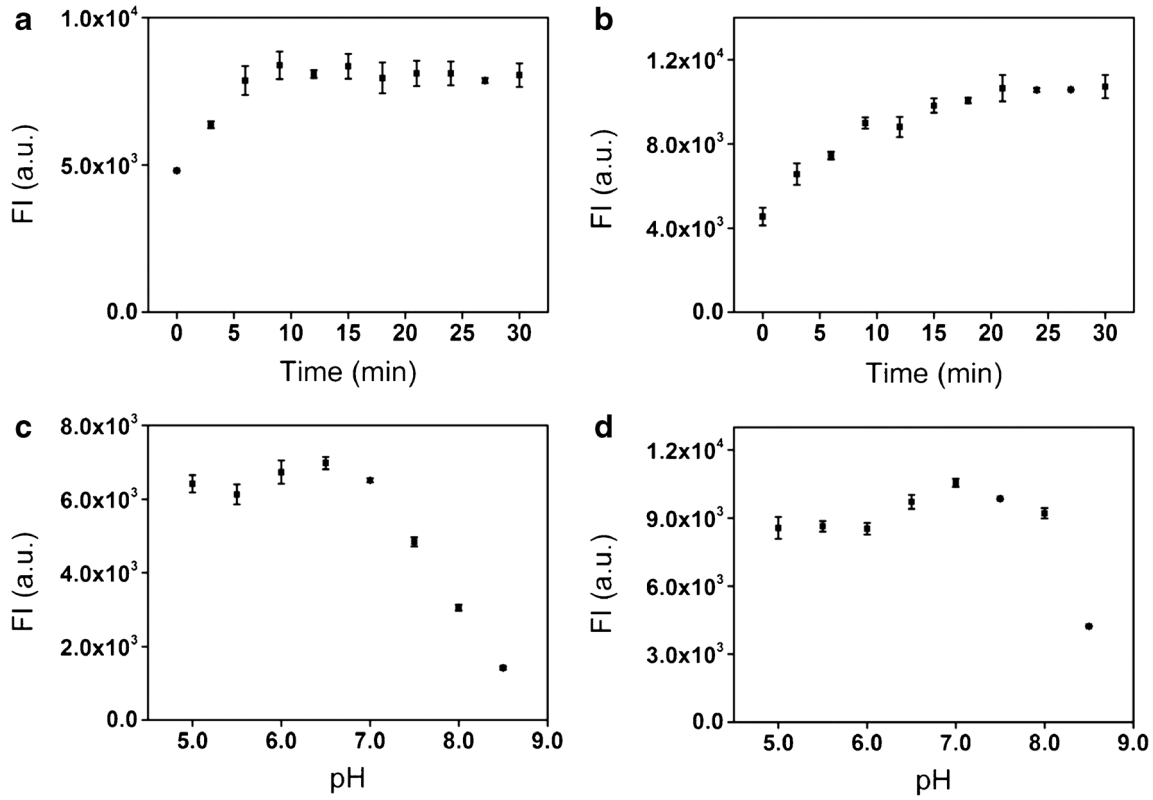

Fig. 3 Effects of reaction time on quinoxaline at 425 nm (**a**) and OPDAox at 568 nm (**b**) of the sensing system. Effects of buffer pH on quinoxaline at 425 nm (**c**) and OPDAox at 568 nm (**d**) of the sensing system. Error bars were obtained according to three independent experiments

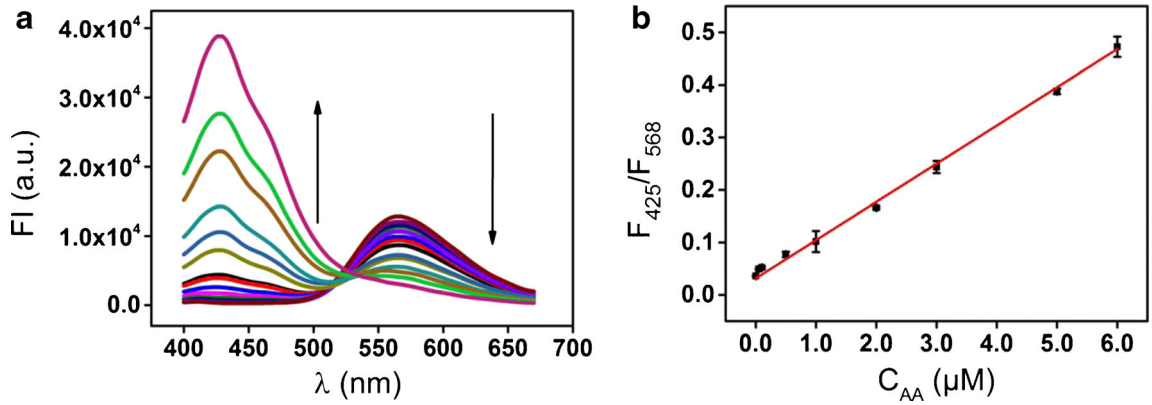

Fig. 4 **a** The fluorescence responses of the sensing system against AA concentration: 0.0, 0.05, 0.1, 0.5, 1.0, 2.0, 3.0, 5.0, 6.0, 10.0, 15.0, 25.0, 30.0, 40.0, 50.0 μM. **b** The linear relationships of F_{425}/F_{568} against AA concentrations. The error bars were obtained according to three independent experiments

MnO_2-NS, the higher the AA concentration is, the more MnO_2-NS is reduced into Mn^{2+}, and the more DHAA is generated, resulting in the fluorescence attenuation of OPDAox and the fluorescence enhancement of quinoxaline. The F_{425}/F_{568} presents linear relationship against AA concentration from 0.0 to 6.0 μM with correlation coefficients of 0.99937. The limit of detection is estimated to be 10 nM according to the calculation of three times of signal to noise, which is comparable or even lower than previous reports for AA determination (see Table S1 in ESM).

The specificity of the developed sensing system

Along with the sensitivity requirement, high specificity is another crucial factor for construction of sensing system. To evaluate the specificity, the potential interferences were tested for mainly organism amino acids, small molecules and metal ions, Fig. 5. The concentration of the interferences was 20 μM, and the concentration of AA was 10 μM. Considering that MnO_2 nanomaterial also can be decomposed by GSH, Cys, and DA, their interferences were specially evaluated. Similar as AA, GSH, Cys, or DA can depress the fluorescence of OPDAox due to the decomposition of MnO_2-NS. However, the product DHAA of AA can transfer non-fluorescent OPDA into fluorescent substrate of quinoxaline, exhibiting fluorescence at 425 nm, which is not found in the case of GSH, DA, and Cys since their products from the interaction with MnO_2 do not interact with OPDA (Fig. 5b). Interestingly, the specific detection of AA can be directly monitored by naked eyes under the UV excitation, which transfers the sensing system from yellow to blue, providing a convenient way for the detection. In previous report, the interference of GSH on AA detection is eliminated by adding mask reagent [26]. In our investigation, the interference can be simply eliminated with the developed ratiometric strategy without using mask reagent. In a mixture of GSH and AA, the concentration of AA can be obtained from the fluorescence response at 425 nm (see Fig. S2 in ESM). The total concentration of mixed GSH and AA can be obtained from the fluorescence response at 568 nm. The concentration of GSH is then calculated according to the difference between F_{568} and F_{425}.

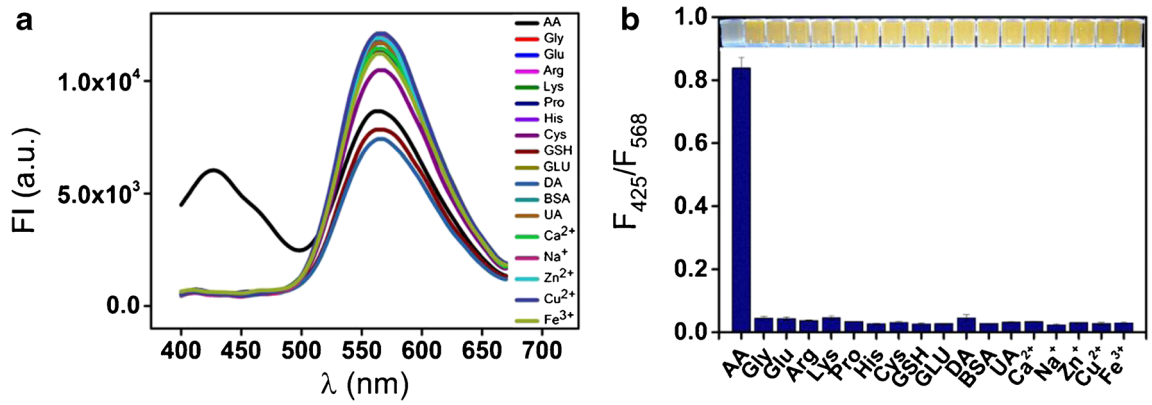

Fig. 5 **a** Fluorescence spectra, **b** F_{425}/F_{568}, and photographs (inset) of the sensing system against AA and the other interfering species. The photographs were taken under UV-radiation (λ_{em} = 302 nm)

Table 1 AA detection in diverse real samples

Sample	Initial amount (μM)	Added amount (μM)	Found amount (μM)	Average recovery (%)	RSD (%, $n = 3$)
Orange juice	2.25	1.0	3.20	95.0	3.5
		2.0	3.98	86.5	2.3
		4.0	5.89	91.0	2.6
Lemon juice	2.17	1.0	3.18	101.0	2.7
		2.0	3.96	89.5	1.6
		4.0	6.01	96.0	2.4
Grapefruit juice	1.86	1.0	3.02	116.0	1.8
		2.0	3.72	93.0	2.2
		4.0	5.49	90.8	3.1
Pineapple juice	1.01	1.0	1.98	97.0	1.2
		2.0	3.07	103.0	2.9
		4.0	4.91	97.5	1.4
Serum	0.22	0.5	0.71	98.0	3.4
		1.0	1.28	106.0	2.7
		3.0	3.06	94.7	3.1

Feasibility of AA detection in real samples

AA widely exists in fruits and vegetables and is usually artificially added into foods and beverages. AA is assimilated into human body via food chain and can be found in cellular fluid of the central nervous system and serum. In the present investigations, serum and diverse beverages including orange juice, lemon juice, grapefruit juice, and pineapple juice were used as model samples to explore the feasibility of AA detection in real sample. AA detection in real samples has been conducted with HPLC. Since the original concentration of AA in the real samples is quite high and is beyond the linear detection range of the as-proposed assay, the real samples were diluted with a certain times to be available for detection with the as-proposed assay. The results obtained with the developed assay are comparable with the HPLC results (see Table S2 in ESM). The feasibility of AA detection in real sample was further explored by spiking a certain amount of AA into the above mentioned samples, which was then qualified following the same procedure of the developed ratiometric assay. Satisfactory recoveries of the spiked AA in beverages are found to be distributed within range from 86.5 to 116%. In serum sample, the recoveries are found within range from 94.7 to 106% (Table 1). The results validate the practical applicability of the developed assay for AA detection in real sample.

Conclusion

A novel ratiometric fluorescent nanosensor has been successfully developed for highly sensitive and selective detection of AA in an enzyme-free and label-free way. The limit of detection reaches as low as 10.0 nM. The developed sensing system presents following advantages. Firstly, the dual fluorescent signals for ratiometric detection were excited with a universal radiation wavelength, simplifying the detection procedure. Secondly, the ratiometric strategy presented excellent selectivity for AA detection, reducing the influence of the external environment, greatly improving the detection accuracy. Specifically the interference from GSH, Cys, and DA can be eliminated without using mask reagent. Satisfactory recoveries were found for monitoring AA levels in serum and beverage samples. Thirdly, the developed assay is quite simple in preparation and operation and can be completed within half an hour, offering a convenient and effective "mix-then-test" way for rapid detection. The proposed assay brings a charming way for cost-effective detection in real samples with excellent repeatability and reliability.

Funding information This work is supported by the National Natural Science Foundation of China (No. 21575138 and No. 21775108), the China International Science and Technology Cooperation Based of Food Nutrition/Safety and Medicinal Chemistry, the Tianjin Municipal Science and Technology Commission (Project No. 16PTSYJC00130), and the International Science and Technology Cooperation Program of China (Project No. 2014DFR30350).

Compliance with ethical standards

Conflict of interest The authors declare that they have no competing interests.

References

1. Nam H, Kwon J, Choi M, Seo J, Shin S, Kim S, et al. Highly sensitive and selective fluorescent probe for ascorbic acid with a broad detection range through dual-quenching and bimodal action of nitronyl-nitroxide. ACS Sensors. 2016;1:392–8.
2. Eggersdorfer M, Laudert D, Létinois U, McClymont T, Medlock J, Netscher T, et al. One hundred years of vitamins-a success story of the natural sciences. Angew Chem Int Ed. 2012;51:12960–90.

3. Zhao P, He K, Han Y, Zhang Z, Yu M, Wang H, et al. Near-infrared dual-emission quantum dots-gold nanoclusters nanohybrid via co-template synthesis for ratiometric fluorescent detection and bioimaging of ascorbic acid in vitro and in vivo. Anal Chem. 2015;87:9998–10005.
4. Liu H, Na W, Liu Z, Chen X, Su X. A novel turn-on fluorescent strategy for sensing ascorbic acid using graphene quantum dots as fluorescent probe. Biosens Bioelectron. 2017;92:229–33.
5. Frajese GV, Benvenuto M, Fantini M, Ambrosin E, Sacchetti P, Masuelli L, et al. Potassium increases the antitumor effects of ascorbic acid in breast cancer cell lines in vitro. Oncol Lett. 2016;11:4224–34.
6. Bi H, Duarte CM, Brito M, Vilas-Boas V, Cardoso S, Freitas P. Performance enhanced UV/vis spectroscopic microfluidic sensor for ascorbic acid quantification in human blood. Biosens Bioelectron. 2016;85:568–72.
7. Figueroa-Méndez R, Rivas-Arancibia S. Vitamin C in health and disease: its role in the metabolism of cells and redox state in the brain. Front Physiol. 2015;6:397.
8. Meng H, Yang D, Tu Y, Yan J. Turn-on fluorescence detection of ascorbic acid with gold nanolcusters. Talanta. 2017;165:346–50.
9. Zhu X, Zhao T, Nie Z, Liu Y, Yao S. Non-redox modulated fluorescence strategy for sensitive and selective ascorbic acid detection with highly photoluminescent nitrogen-doped carbon nanoparticles via solid-state synthesis. Anal Chem. 2015;87:8524–30.
10. Li L, Wang C, Liu K, Wang Y, Liu K, Lin Y. Hexagonal cobalt oxyhydroxide-carbon dots hybridized surface: high sensitive fluorescence turn-on probe for monitoring of ascorbic acid in rat brain following brain ischemia. Anal Chem. 2015;87:3404–11.
11. Ji D, Du Y, Meng H, Zhang L, Huang Z, Hu Y, et al. A novel colorimetric strategy for sensitive and rapid sensing of ascorbic acid using cobalt oxyhydroxide nanoflakes and 3, 3′, 5, 5′-tetramethylbenzidine. Sensors Actuators B Chem. 2018;256:512–9.
12. Feng L, Wu Y, Zhang D, Hu X, Zhang J, Wang P, et al. Near infrared graphene quantum dots-based two-photon nanoprobe for direct bioimaging of endogenous ascorbic acid in living cells. Anal Chem. 2017;89:4077–84.
13. Wang H, Pu G, Devaramani S, Wang Y, Yang Z, Li L, et al. Bimodal electrochemiluminescence of G-CNQDs in the presence of double coreactants for ascorbic acid detection. Anal Chem. 2018;90:4871–7.
14. Lima DRS, Cossenza M, Garcia CG, Portugal CC, de C Marques FF, Paes-de-Carvalho R, et al. Determination of ascorbic acid in the retina during chicken embryo development using high performance liquid chromatography and UV detection. Anal Methods. 2016;8:5441–7.
15. Lin X, Liu Y, Tao Z, Gao J, Deng J, Yin J, et al. Nanozyme-based bio-barcode assay for high sensitive and logic-controlled specific detection of multiple DNAs. Biosens Bioelectron. 2017;94:471–7.
16. Lin X, Liu Y, Deng J, Lyu Y, Qian P, Li Y, et al. Multiple advanced logic gates made of DNA-Ag nanocluster and the application for intelligent detection of pathogenic bacterial genes. Chem Sci. 2018;9:1774–81.
17. Han Q, Dong Z, Tang X, Wang L, Ju Z, Liu W. A ratiometric nanoprobe consisting of up-conversion nanoparticles functionalized with cobalt oxyhydroxide for detecting and imaging ascorbic acid. J Mater Chem B. 2017;5:167–72.
18. Rong M, Lin L, Song X, Wang Y, Zhong Y, Yan J, et al. Fluorescence sensing of chromium (VI) and ascorbic acid using graphitic carbon nitride nanosheets as a fluorescent "switch". Biosens Bioelectron. 2015;68:210–7.
19. Zhai W, Wang C, Yu P, Wang Y, Mao L. Single-layer MnO_2 nanosheets suppressed fluorescence of 7-hydroxycoumarin: mechanistic study and application for sensitive sensing of ascorbic acid in vivo. Anal Chem. 2014;86:12206–13.
20. Fan S, Zhao M, Ding L, Li H, Chen S. Preparation of Co3O4/crumpled graphene microsphere as peroxidase mimetic for colorimetric assay of ascorbic acid. Biosens Bioelectron. 2017;89:846–52.
21. Zheng M, Xie Z, Qu D, Li D, Du P, Jing X, et al. On-off-on fluorescent carbon dot nanosensor for recognition of chromium (VI) and ascorbic acid based on the inner filter effect. ACS Appl Mater Interfaces. 2013;5:13242–7.
22. Luo X, Zhang W, Han Y, Chen X, Zhu L, Tang W, et al. S co-doped carbon dots based fluorescent "on-off-on" sensor for determination of ascorbic acid in common fruits. Food Chem. 2018;258:214–21.
23. Liu R, Yang R, Qu C, Mao H, Hu Y, Li J, et al. Synthesis of glycine-functionalized graphene quantum dots as highly sensitive and selective fluorescent sensor of ascorbic acid in human serum. Sensors Actuators B Chem. 2017;241:644–51.
24. Hu L, Deng L, Alsaiari S, Zhang D, Khashab NM. "Light-on" sensing of antioxidants using gold nanoclusters. Anal Chem. 2014;86:4989–94.
25. Li N, Li Y, Han Y, Pan W, Zhang T, Tang B. A highly selective and instantaneous nanoprobe for detection and imaging of ascorbic acid in living cells and in vivo. Anal Chem. 2014;86:3924–30.
26. Cen Y, Tang J, Kong X, Wu S, Yuan J, Yu R, et al. A cobalt oxyhydroxide-modified upconversion nanosystem for sensitive fluorescence sensing of ascorbic acid in human plasma. Nanoscale. 2015;7:13951–7.
27. Meng H, Zhang X, Yang C, Kuai H, Mao G, Gong L, et al. Efficient two-photon fluorescence nanoprobe for turn-on detection and imaging of ascorbic acid in living cells and tissues. Anal Chem. 2016;88:6057–63.
28. Deng R, Xie X, Vendrell M, Chang Y, Liu X. Intracellular glutathione detection using MnO_2-nanosheet-modified upconversion nanoparticles. J Am Chem Soc. 2011;133:20168–71.
29. Dong Z, Lu L, Ko C, Yang C, Li S, Lee M, et al. A MnO_2 nanosheet-assisted GSH detection platform using an iridium (iii) complex as a switch-on luminescent probe. Nanoscale. 2017;9:4677–82.
30. Fan H, Zhao Z, Yan G, Zhang X, Yang C, Meng H, et al. A smart DNAzyme-MnO_2 nanosystem for efficient gene silencing. Angew Chem Int Ed. 2015;12:4883–7.
31. Xiao T, Sun J, Zhao J, Wang S, Liu G, Yang X. FRET effect between fluorescent polydopamine nanoparticles and MnO_2 nanosheets and its application for sensitive sensing of alkaline phosphatase. ACS Appl Mater Interfaces. 2018;10:6560–9.
32. Omomo Y, Sasaki T, Wang L, Watanabe M. Redoxable nanosheet crystallites of MnO_2 derived via delamination of a layered manganese oxide. J Am Chem Soc. 2003;125:3568–75.
33. Fan D, Shang C, Gu W, Wang E, Dong S. Introducing ratiometric fluorescence to MnO_2 nanosheet-based biosensing: a simple, label-free ratiometric fluorescent sensor programmed by cascade logic circuit for ultrasensitive GSH detection. ACS Appl Mater Interfaces. 2017;9:25870–7.
34. Liu J, Meng L, Fei Z, Dyson P, Jing X, Liu X. MnO_2 nanosheets as an artificial enzyme to mimic oxidase for rapid and sensitive detection of glutathione. Biosens Bioelectron. 2017;90:69–74.
35. Han L, Liu S, Zhang X, Tao B, Li N, Luo H. A sensitive polymer dots-manganese dioxide fluorescent nanosensor for "turn-on" detection of glutathione in human serum. Sensors Actuators B Chem. 2018;258:25–31.
36. Kong X, Wu S, Chen T, Yu R, Chu X. MnO_2-induced synthesis of fluorescent polydopamine nanoparticles for reduced glutathione sensing in human whole blood. Nanoscale. 2016;8:15604–10.
37. Lin Z, Li M, Lv S, Zhang K, Lu M, Tang D. In situ synthesis of fluorescent polydopamine nanoparticles coupled with enzyme-controlled dissolution of MnO_2 nanoflakes for a sensitive immunoassay of cancer biomarkers. J Mater Chem B. 2017;5:8506–13.

38. Guo B, Pan X, Liu Y, Nie L, Zhao H, Liu Y, et al. A reversible water-soluble naphthalimide-based chemosensor for imaging of cellular copper (II) ion and cysteine. Sensors Actuators B Chem. 2018;256:632–8.
39. Lu H, Xu S. Visualizing BPA by molecularly imprinted ratiometric fluorescence sensor based on dual emission nanoparticles. Biosens Bioelectron. 2017;92:147–53.
40. Zhang X, Zheng C, Guo S, Li J, Yang H, Chen G. Turn-on fluorescence sensor for intracellular imaging of glutathione using g-C3N4 nanosheet–MnO_2 sandwich nanocomposite. Anal Chem. 2014;86:3426–34.
41. Hu Y, Zhang L, Geng X, Ge J, Liu H, Li Z. A rapid and sensitive turn-on fluorescent probe for ascorbic acid detection based on carbon dots–MnO_2 nanocomposites. Anal Methods. 2017;9:5653–8.
42. Chung HK, Ingle JD Jr. Fluorimetric kinetic method for the determination of total ascorbic acid with *o*-phenylenediamine. Anal Chim Acta. 1991;243:89–95.